Synthetic and Systems Biotechnology 5 (2020) 206–213

Contents lists available at ScienceDirect

Synthetic and Systems Biotechnology

journal homepage: http://www.keaipublishing.com/synbio

Positional assembly of multi-enzyme cascade reaction in polyelectrolyte doped microcapsule through electrospray and layer-by-layer assembly

Shiyi Che[a,b,1], Jie Wang[a,c,1], Xiaoyuan Ji[a], Zhiguo Su[a], Shaomin Wang[c,**], Songping Zhang[a,*]

[a] State Key Laboratory of Biochemical Engineering, Institute of Process Engineering, Chinese Academy of Sciences, Beijing, 100190, China
[b] University of Chinese Academy of Sciences, No. 19 Yuquan Road, Shijingshan District, Beijing, 100049, China
[c] College of Chemistry, Zhengzhou University, Zhengzhou, 450001, China

ARTICLE INFO

Keywords:
Coaxial electrospray
Microcapsule
Multi-enzyme
Cascade reaction
Positional assembly
Layer-by-layer assembly

ABSTRACT

Polyelectrolyte-doped microcapsules (PDM) was fabricated by coaxial electrospray of a mixture of glycerol and water containing 10 mg/mL cationic polyelectrolyte poly(allylamine hydrochloride) (PAH) fed as the core phase solution, and a N,N-dimethylacetylamide solution of 10 wt% polyurethane fed as the shell phase solution. Multi-enzyme system involving Candida Antarctica lipase B (CALB), glucose oxidase (GOD), and horseradish peroxidase (HRP) for cascade reaction was assembled in the PDM at three different places, namely, surface, shell, and lumen. Placing of enzyme inside aqueous lumen of the PDM was realized by *in situ* encapsulation through adding the enzyme in the core-phase solution for coaxial electrospray. By ion-pairing of enzyme with cationic surfactant CTAB, an organic soluble enzyme-CTAB complex was prepared, so that *in situ* embedding of enzyme in the shell of the PDM was realized by adding it into the shell phase solution. Surface attachment of enzymes was achieved by layer-by-layer (LbL) technology, which is based on the ion-exchange interactions between oppositely charged enzymes and PAH that was doped in PDM. The enzyme-decorated microcapsule was then studied as a micro-bioreactor, in which 1-Oxododecyla-α-glucopyranoside was converted by CALB to glucose, which was oxidised by GOD to gluconolactone in a second step. The hydrogen peroxide produced was then used by HRP to oxidize ABTS to form coloured radical cation $ABTS^{\bullet+}$ for activity analysis. The successful fabrication of the PDM and precise localization of enzymes in the PDM by different strategies were fully characterized. By varying the immobilization strategy, totally six PDM bioreactors with three enzymes precisely positional assembled in different strategies were constructed and their activities for the cascade reaction were investigated and compared. The PDM micro-bioreactor prepared by novel electrospray technologies provide a smart platform for positional assembly of multi-enzyme cascade reaction in a precise and well-controlled manner.

1. Introduction

Cascade reactions catalyzed by multienzymatic system have been at the leading edge of biocatalysis development because of their unique advantages in reaction route flexibility, less side reaction, and high atom economy and reaction efficiency [1,2]. From the *in vitro* fixation of CO_2 [3] to the multi-step biocatalytic cascade for the manufacture of anti-HIV drug islatravia [4], considerable progresses have been made in recent years to develop cell-free complex multienzyme catalysis reactions in the laboratory. To make these impressive progresses into practice applications, efficient strategies for immobilization, compartmentalization and co-localization of the multienzymatic system become highly demanded, but challenging [1]. In living cells, compartmentalization is the most fascinating feature so that the complicated biochemical reaction can be precisely controlled by enzymes, each of which is localized at the specific place [2,5–8]. Inspired by nature's ingenuity, design of synthetic microcapsule with single or multi-compartments that can effectively co-localize the multienzymes is the most critical issue to reduce the incompatibility limitation and regulate the time and space of the reactions.

Liposomal microcapsules [9] and semipermeable microcapsules [10] are among the earliest carriers reported for multienzymes, however, they are too fragile to be practically operated. Synthetic porous polymersomes with good mechanical strength based on block

Peer review under responsibility of KeAi Communications Co., Ltd.
* Corresponding author.
** Corresponding author.
E-mail addresses: wshaomin@zzu.edu.cn (S. Wang), spzhang@ipe.ac.cn (S. Zhang).
[1] Both authors contributed equally to this work.

https://doi.org/10.1016/j.synbio.2020.06.010
Received 31 March 2020; Received in revised form 6 June 2020; Accepted 27 June 2020

copolymers were successfully synthesized for a three-enzyme cascade reaction through positional assembly of the enzymes at three different locations, namely, in their lumen, in their bilayer membrane and on their surface. Nevertheless, both the enzyme loading capacity and the overall reaction efficiency were unsatisfactory, due to the poor permeability of polymersomes and the deactivation of enzyme by polar organic solvent tetrahydrofuran during the synthetic process [6,11]. Many other different microcapsules and vesicles with complicated multi-level structures had been constructed and applied, such as shell-in-shell microcapsules [12], stomatocytes-like bi-enzyme nanomotor, polymeric colloidosomes [8], double membrane microcapsules [13] et al. Most of the fabrication process, however, are rather complicated. For instance, to make double membrane microcapsules for multienzyme immobilization, $CaCO_3$ and SiO_2 were used as double sacrificial templates and totally 7 steps including bioinspired silicification and layer-by-layer assembly were involved [13]. Therefore, developing new materials suitable for multienzyme assembly is appealing.

Electrospinning is a versatile and viable technique for generating ultrathin fibers put forward as early as 1934, since then remarkable progress has been made with regard to the development of electrospinning methods and engineering of electrospun nanofibers to suit or enable various applications using as “smart” mats, filtration membranes, catalytic supports, energy harvesting/conversion et al. [14]. The concentration of polymer solution is one of the significant factors that influence nanofiber's shapes and dimensions, as low concentration leads to fibers with beads arranged like a string of pearls. An extreme end of beads are microspheres, which are formed during the electrospinning under appropriate conditions, such as concentration, viscosity and distance between needle and collector. In that case, this method to manufacture microsphere, is named as electrospray [15]. Instead of continuous non-woven fibers, discrete microspheres will be formed.

Recently, a unique co-axial electrospinning or electrospray technology was developed by our group, through which hollow nanofibers or microcapsules were fabricated by using a mixture of glycerol and water as the core phase solution, and a polymer solution in an organic solvent as the shell phase solution [16–19]. By simply adding enzymes into the core-phase solution, *in situ* encapsulation of enzymes inside the lumen of the hollow nanofibers were realized. Further supplementing a cationic polyelectrolyte poly(allylamine hydrochloride) (PAH) in the core phase solution enabled attachment of enzyme onto the surface of the nanofibers *via* ion-exchange interaction between the enzyme and the PAH, which is doped in the materials [18–20]. This hollow nanofiber provides a versatile platform for construction of a variety of multienzyme systems, even that for five-enzymes-cofactor catalyst system catalyzing bioconversion of carbon dioxide to methanol [18]. Significant advantages like mild preparation condition, nanoconfinedeffect to stabilize enzymes, 100% loading efficiency by *in situ* encapsulation, positional assembly of multienzymes et al., have been demonstrated.

In this present work, we aim to further broaden the application and explore the feasibility of this microcapsule fabricated by coaxial electrospray in positional assembly of multi-enzyme cascade reaction. The proposed strategy is schematically depicted in Fig. 1. The three-enzyme system for cascade reaction includes *Candida Antarctica* lipase B (CALB), glucose oxidase (GOD), and horseradish peroxidase (HRP). Polyelectrolyte-doped microcapsules (PDM) will be fabricated by coaxial electrospray, using a mixture of glycerol and water containing PAH as the core phase solution, and N, N-dimethylacetylamide (DMAc) solution of polyurethane as the shell phase solution. The three enzymes will be assembled in the PDM at three different places, namely, surface, shell, and lumen. Placing of CALB inside aqueous lumen of the PDM will be realized by *in situ* encapsulation through adding the enzyme in the core-phase solution for coaxial electrospray. While an ion-pairing of enzyme with cationic surfactant CTAB will be conducted to get organic soluble GOD-CTAB complex [21,22], so that the GOD can be *in situ* embedded in the shell of the PDM. The third enzyme HRP will be attached to the outer surface of the PDM by layer-by-layer (LbL) technology, which is based on the ion-exchange interactions between oppositely charged enzymes and PAH that was doped in PDM.

The enzyme-decorated microcapsule was then studied as a nanoreactor, in which 1-Oxododecyla-α-glucopyranoside was converted by CALB to glucose, which was oxidised by GOD to gluconolactone in a second step. The hydrogen peroxide produced was then used by HRP to oxidize ABTS to form coloured radical cation $ABTS^{\bullet+}$ for activity analysis. The fabrication of the PDM and precise localization of enzymes in the PDM by different strategies will be fully characterized. And effect of different spatial positions of the enzymes in the cascade reaction will be investigated and compared.

2. Materials and methods

2.1. Materials

Candida antarctica lipase B (CALB, EC.3.1.1.3, recombinant expressed in *Aspergillus Niger*), Glucose Oxidase from *Aspergillus Niger* (GOD, EC.1.1.3.4), Peroxidase from horseradish (HRP, EC.1.11.1.7), Poly(allylamine hydrochloride) (PAH, MW: ~200 kDa), p-Nitrophenol, 2,2′-Azinobis-(3-ethylbenzthiazoline-6-sulphonate) (ABTS), Fluorescamine, were purchased from Sigma-Aldrich chemical. Sulforhodamine 101 and FITC were purchased from Aladdin. D-glucose anhydrous, hexadecyl trimethyl ammonium bromide (CTAB), N, N-Dimethylacetylamide (DMAc), glycerol were purchased from Beijing Chemical Factory, 1-Oxododecyla-α-glucopyranoside was purchased from Beijing Saenke Biotechnology Company, Hydrogen peroxide was purchased from Beijing Xinjingke Biotechnology Company, Polyurethane A85E pellets with a bulk density of approximately 700 kg/m^3 was supplied by Xiamen Jinyouju Chemical Agent (Xiamen China).

2.2. Preparation of organic solvent soluble enzyme by ion-pairing

Briefly, 1 mg/mL of enzyme solution prepared in 50 mM phosphate buffer (pH 7.0) containing 20 mM KCl was blended with an equal volume of n-octane and n-hexanol (v/v = 4:1) containing 2 mM CTAB. The mixed solution was homogenized by rapid magnetic stirring for 3 min and then centrifuged for 5 min 6000 rpm. To recover the CTAB-enzyme complex in the bottom, the top layer organic solution was dried by blowing N_2. To optimize the ion-pairing process, the pH of buffer solution, concentration for KCl and CTAB was varied.

2.3. Preparation of PAH-doped PU microcapsules by co-axial electrospray for in situ encapsulation/doping of enzymes

PAH-doped PU microcapsules (PDM) was prepared by co-axial electrospray following procedures as described in our previous work [19] with slight modification. Briefly, the shell-phase solution of electrospray consists of a 10 wt % PU solution in DMAc. A mixture solution of 200 μL buffer and 800 μL glycerol containing 10 mg PAH was used as the core-phase solution of coaxial electrospray. The coaxial electrospray was conducted at 25 ± 3 °C, 10–15% humidity. The core solution and shell solution were fed through two syringe pumps at a flow rate of 0.05 mL/h and 1.0 mL/h, respectively. A positive voltage of 20 kV was applied and an aluminum sheet was used as the collector at a distance of 30 cm away from the nozzle tip.

By directly adding about 1 mg enzyme to the core phase solution, the enzyme can be *in situ* encapsulated inside the lumen of the microcapsules. While *in situ* embedding of enzyme in the PU shell of microcapsules was realized by directly adding the organic soluble enzyme-CTAB complex into the shell phase solution. By adding one enzyme into core phase solution and another one into the shell phase solution simultaneously, microcapsules with positional assembled enzymes in the shell and inside aqueous lumen of microcapsule were fabricated in one step during electrospray.

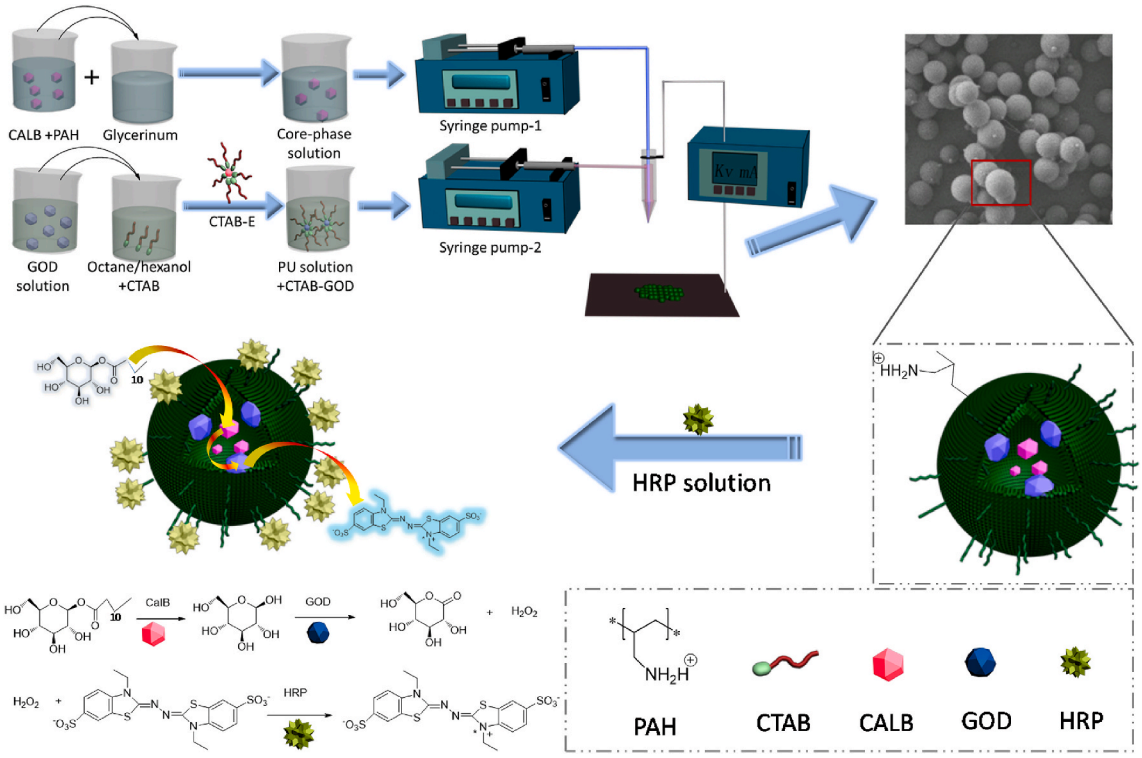

Fig. 1. Schematic illustration of the setup for coaxial electrospray for constructing PAH-doped microcapsule for precisely positional assembly of three-enzyme cascade reaction.

2.4. Assembly of enzyme on surface of PDM by LBL self-assembly

To immobilize enzyme on the outer surface of the PDM via ion-exchange interactions, about 5 mg microcapsules were incubated into 1 mg/mL enzyme solution (1 mL, 50 mM, pH 7.0). After incubation at 4 °C for 15 min, the microcapsules were taken out from the solution by centrifuging and washed three times with fresh PBS buffer. The loading amount of enzyme was calculated via mass balance.

2.5. Construction of three-enzyme cascade reaction system

Based on above methods, totally six PDM bioreactors were constructed by precisely positional assembly of the three enzymes in different positions, namely: (1) lumen (CALB) + shell (GOD)-surface (HRP), (2) lumen (GOD) + shell (CALB)-surface (HRP), (3) lumen (GOD) + shell (HRP)-surface (CALB), (4)lumen (HRP) + shell (GOD)-surface (CALB), (5) lumen (CALB) + shell (HRP)-surface (GOD), and (6) lumen (HRP) + shell (CALB)-surface (GOD).

2.6. Characterization

The morphologies of the microcapsules were characterized by scanning electronic microscopy (SEM, JSM-6700F, JEOL, Japan) after sprayed gold on the surface. To verify the hollow structures of microcapsules, the microcapsules were characterized by Transmission Electron Microscope (TEM, JEM-2100UHR, JEOL, Japan), and approximately 100 different microcapsules were analyzed to determine their size distribution of the inner and outer diameters. Hydrophobicity of the microcapsules was evaluated using a contact angle instrument (DSA100, Kruss, Germany).

In order to characterize the localization of different enzymes in the PDM bioreactor, HRP, GOD, and CALB were pre-labeled by FITC, Sulforhodamine, and Fluorescamine, respectively, prior to being assembled on the outer surface, in the shell and inside lumen of the microcapsules. The microcapsules were characterized by confocal laser scanning microscopy (CLSM) with Leica TCS SP5 microscope (Leica Camera AG, Germany). The laser provided excitation of Sulforhodamine 101 at 586 nm and emitted fluorescent light was detected at 605 nm. Similarly, FITC (ex 488 nm, em 525 nm) and Fluorescamine (ex 395 nm em 475 nm) were observed.

2.7. Loading amount and activity measurement of enzymes

The total loading amount of multi-enzyme system microcapsules at the core-shell solution flow rate of 0.05: 1 mL/h was calculated as follows. The microcapsules in receiver board were weighted after 0.5 h during the electrospray, thus the solution consumption of core and shell phase were calculated as 0.025 mL and 0.5 mL. Enzyme concentrations in core and shell solution were known to figure out the loading amount. Amount of enzymes loaded through LBL was determined by comparing the initial and final concentration of enzymes after immobilization.

Activity of CALB was determined by measuring the initial hydrolysis rate of p-NPA to p-nitrophenol at pH 7.0 and 25 °C, which was monitored by measuring the absorbance at 410 nm (A_{410}, $\varepsilon^{p\text{-}nitrophenol} = 24.9\ mM^{-1}\ cm^{-1}$) every 30 s interval and lasted for 5 min. Activity unit of GOD was defined as the amount of enzyme needed to oxidize 1 μM glucose to glucose-lactone in 1 min at pH 7.0 and 25 °C, which was monitored by measuring the absorbance at 420 nm (A420, $\varepsilon^{ABTS} = 36\ mM^{-1}\ cm^{-1}$) continuously for 3 min using a Unico 2800 spectrophotometer. Detailed conditions for activity measurement were described in our previous work [20].

Activity unit of HRP was defined as the amount of enzyme needed to oxidize 1 μM H_2O_2 to H_2O in 1 min at pH 7.0 and 25 °C. To initiate the reaction, free HRP (0.5 μg/mL) or microcapsule containing HRP was added to sodium phosphate buffer solution (1 mL, 50 mM, pH = 7.0) containing H_2O_2 (0.1 mol/mL) and ABTS (0.3 mg/mL). The reaction was monitored by measuring the absorbance at 420 nm with the same methods as above described.

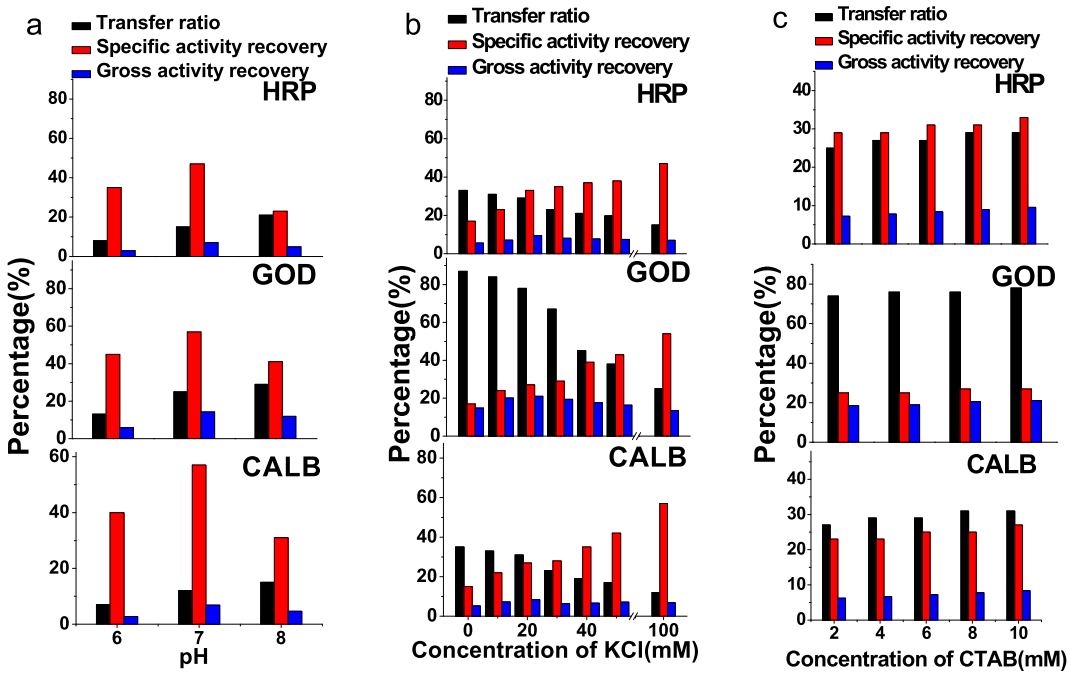

Fig. 2. Optimization of ion-pairing process for preparation of organic solvent soluble enzyme-CTAB complex. a) The effect of pH in buffer solution on transfer rate (TR), specific activity recovery (SAR) and gross activity recovery (GA) of HRP, GOD and CALB. The concentrations of KCl, CTAB and enzyme were 100 mM, 10 mM, and 1 mg/mL, respectively. b) The effect of KCl concentration on TR, SAR and GA of HRP, GOD and CALB. The buffer pH was 7.0, concentrations of CTAB and enzyme was 10 mM, and 1 mg/mL, respectively. c) The effect of CTAB concentration on TR, SAR and GA of HRP, GOD and CALB. The buffer pH was 7.0, concentrations of KCl and enzyme was 20 mM, and 1 mg/mL, respectively.

2.8. Three-enzyme cascade reaction

The reactant of three-enzyme cascade reaction system was composed of 0.2 mg/mL 1-Oxododecyla-α-glucopyranoside and 0.3 mg/mL ABTS in 50 mM phosphate buffer solution (2 mL, pH 7.0). The reaction was initiated by adding microcapsules (about 10 mg) with positional assembly of three-enzymes or free enzymes with dosage equivalent to that in microcapsules. The reaction was monitored by measuring the formation of $ABTS^{\cdot+}$ by its absorbance at 420 nm (A420, ε^{ABTS} = 36 $mM^{-1}cm^{-1}$) continuously for 3 min using a Unico 2800 spectrophotometer. For the activity measurement of microcapsules multi-enzyme system, A_{420} was measured at every 30 s after filtering the microcapsules with syringe filter.

The three-enzyme cascade reaction catalyzed by the microcapsule bioreactors with positional assembly enzymes in six different positions (see section 2.4) were tested following the same procedure, and their activity recoveries were calculated by comparing the $ABTS^{\cdot+}$ formation rate catalyzed by the microcapsule bioreactor with that by free enzymes with same dosage.

2.9. Thermal and operational stabilities of the multi-enzyme system

Thermal stability of the immobilized multi-enzyme systems was determined by measuring changes in the initial reaction rate of cascade reaction after the multi-enzyme microcapsules were incubated at 60 °C for different times. Operational stability of the immobilized multi-enzyme systems was examined by measuring the reaction rate of the cascade reaction after several repeated usages. The reactions were run for 3 min before they were stopped by centrifuging the microcapsules. After washing the microcapsule with buffer solution, fresh substrates including 1-Oxododecyla-α-glucopyranoside and ABTS were added, and the next reaction measurement was carried out. The reaction rate of the multi-enzyme systems in the first time was defined as 100%.

3. Results and discussion

3.1. Optimization of the preparation of organic soluble enzyme

The objective of this study was to position enzymes at three specific locations within or on a microcapsule, namely inside lumen, in its shell, and on its surface. Since the PU shell phase solution to form shell of PU microcapsule was prepared in an organic solvent. Therefore, the enzyme to be doped in the PU shell must be organic soluble. An ionpairing strategy based on electrostatic interactions between the positively charged enzyme and negatively charged anionic surfactant AOT had been used to prepare AOT-enzyme complex, which became organic solvent soluble [21]. Here in the recent work, the isoelectric point of all the three enzymes in the cascade reaction were all below 7.0 (CALB 4.2, GOD 3.8, HRP 4.1). When AOT was used to solubilize the enzymes, only less than 10% enzyme was transferred to organic solvent phase (data not shown). Therefore a cationic surfactant CTAB was substituted for the anionic surfactant AOT to ensure the formation of enzyme-CTAB complex at the neutral pH conditions.

To find out the optimal condition to make organic soluble enzyme by forming enzyme-CTAB through ion-pairing, the experimental parameters including pH, KCl concentration in aqueous solution, and the CTAB concentration in organic phase were optimized for each of the three enzymes. The transfer ratio (TR) was defined as the percentage of enzyme transferred from aqueous phase to organic phase, which was determined by comparing the initial and final enzyme concentration in aqueous phase after ion-pairing. The specific activity recovery (SAR) of the ion-pairing enzymes recovered from organic phase was calculated by comparing the specific activity of the enzyme-CTAB complex with that of the free enzyme; while the gross activity recovery (GAR) was defined as the ratio of total activity recovered from organic phase to the total enzyme activity initially put in the aqueous phase.

According to results presented in Fig. 2a, the TR of all the three enzymes increased as increase of pH, due to enhanced electrostatic interactions between enzyme and CTAB at higher pH. The highest SAR

were obtained at pH 7.0, which was mainly related to the optimal pH for enzyme. The highest GAR was also obtained at pH 7.0. In order to obtain as much bioactive organic soluble enzyme as possible, the GAR was considered the most important, therefore pH 7.0 was chosen as the optimum pH for ion-pairing process.

Fig. 2b presents the effect of KCl concentration on the ion-pairing process. The TR significantly declined as increase of KCl, because the electrostatic interactions between enzyme and CTAB were weakened by high ionic strength. While the SAR of enzymes positively correlated to concentration of KCl, which might protect the enzyme from deactivation upon contact with organic solvent. A KCl concentration of 20 mM compromised this contradictory issue mostly, under which condition an optimal GAR was obtained. The ion-pairing efficiency was also affected by CTAB concentration (Fig. 2c), higher CTAB concentration seemed to be slightly favorable to the process. However, the CTAB-enzyme complex prepared by the CTAB concentration higher than 2 mM was found to cause serious deformation of the droplets and instability of the electric field around the droplets during later-on electrospray, therefore the CTAB concentration was set for 2 mM. It was noted that in most cases, the enzyme lost nearly 50% of its specific activity after forming enzyme-CTAB complex. Besides organic solvent caused enzyme deactivation, the poor dispersion of the formed enzyme-CTAB complex in activity assay reactant solution could also lead to the low activity recovery. Taking together, the optimal concentration for ion-pairing was pH 7.0, 20 mM KCl and 2 mM CTAB, under this condition, the GAR of GOD, HRP and CALB was 25%, 8.5% and 6.9%, respectively.

3.2. Preparation and characterization of PDM based three-enzyme bioreactor

As a first step towards the three-enzyme cascade system, PU microcapsule loaded with one enzyme in their shells and another one in their aqueous lumen were prepared by coaxial electrospray technology. In our previous work, PAH-doped PU continuous nanofibers have been successfully fabricated by coaxial electrospinning [20]. By manipulating the conditions of the co-axial electrospinning process, for example, by lowering the PU concentration from 25 wt% to 10 wt% and adjusting the flow rate of the electrospinning solution, the electrospinning process changed to an electrospray operation. Under optimized conditions, discrete microcapsules with uniform size were successfully prepared.

Fig. 3 presents the SEM images the as-prepared PDM, for comparison, pure PU microcapsules without PAH were also prepared and characterized. We can see that the morphology of microcapsules was almost unaffected by addition of 10 mg/mL PAH in the core-phase solution. Both microcapsules had uniform size, with average inner diameter of 3.5 μm and outer diameter of 5 μm based on TEM characterization of approximately 100 microcapsules. The contact angle of pure PU microcapsules was 135.1 °C, and this value was decreased to 120.4 °C after PAH doped, which indicated that PAH was not only encapsulated in the inner chamber of microcapsules, but also permeated through the shell to the external surface of the microcapsules during the electrospray process, which increased the hydrophilicity of the prepared microcapsules and facilitated the further enzyme attachment *via* electrostatic interaction [20].

Placement of enzymes inside the lumen of the microcapsule was accomplished by *in situ* encapsulation during coaxial electrospraying, and the uniform distribution of the CALB, for example, inside the lumen of the microcapsule were confirmed by the CLSM observation (Figs. 3c-1). PAH which was added in the core-phase solution is a linear cationic polyelectrolyte, it will move to the inner wall of the shell and penetrate across the shell during formation of the microcapsule [18]. Therefore, some of CALB encapsulated inside the lumen tend to be “glued” to the inner wall of the shell due to electrostatic interactions between ionizable groups of PAH and negatively charged enzyme, as shown in Figs. 3c-1. The doping of PAH allowed us to assemble the enzyme on the outer surface *via* these similar electrostatic interactions between oppositely charged enzyme and the PAH, which was one of the most widely used mechanisms of LBL technology. The successful assembly of HRP on the outer surface of PAH-doped microcapsule was clearly confirmed by CLSM observation shown in Fig. 3(c-2) and Fig. 3(c-3). By co-solubilizing the GOD-complex in organic solvent along with the PU polymer, the GOD was *in situ* embedded in the shell of the microcapsules, as shown in Fig. 3(c-4).

Since loading of enzymes inside the lumen and shell of the microcapsule was achieved *in situ* during co-axial electrospraying; therefore, their corresponding loading amount was determined by the enzyme concentrations (C_{inner}) in the inner-phase or outer-phase solutions (C_{inner}) for co-axial electrospray, as well as their feeding flow rates, which are 0.05 and 1 mL/h, respectively. For example, after 1 h stable co-axial electrospraying, the enzyme encapsulated inside the lumen will be C_{inner} (mg/mL)*0.05 (mL/h) * 1(h); similarly, the enzyme embedded in the shell can be calculated from its concentration in outer-phase solution and its feeding flow rate, i.e., C_{outer} (mg/mL)*1.0 (mL/h)* 1 (h). By weighing the weight of the microcapsules collected on the receiver during 1 h's electrospray, the enzyme loading capacity in per gram of microcapsule was then calculated. While for the enzyme assembled on outer surface of the microcapsule, its capacity was experimental determined by comparing the enzyme concentration before and after adsorption. The loading capacities of CALB, GOD, and HRP assembled in different positions of the microcapsules, as well as their activities were determined, results were listed in Table 1. It was noted that the loading capacity of GOD on the surface of PDM was significantly lower than the other two enzymes, it was considered mainly due to its larger molecular weight of GOD (160 kDa) than CALB and HRP, which is 33 kDa and 43 kDa, respectively.

For all these three enzymes, *in situ* encapsulation inside the aqueous lumen of the microcapsule retained highest activities which are above 75%, compared to the free enzyme under the same conditions. This is due to very mild encapsulation conditions and short diffusional distance for substrates to diffuse across the thin shell of the microcapsule. Enzymes assembled on the surface of microcapsules also showed quite high activities, over 68% for all the enzymes. In situ embedded in the PU shell seems to lead to more significant loss in enzyme activities, about 45–56% activity was recovered, mainly due to organic solvent deactivation and steric hindrance by the polymer shell [20].

3.3. Cascade reaction by microcapsule bioreactor with three enzymes

As described in Section 2.4, totally six microcapsule bioreactors were constructed by incorporating the three enzymes in different strategies. As illustrated by Fig. 1, the cascade reaction involves hydrolysis of 1-Oxododecyla-α-glucopyranoside by CALB to release glucose, which acts as the substrate of GOD. The oxidation of glucose by GOD generates hydrogen peroxide, which was then used by HRP to convert ABTS to coloured radical cation $ABTS^{\bullet+}$.

Loading amount of each enzyme (mg/g-microcapsule) in each of the microcapsule bioreactors was listed in Table 2. To determine the relative activity of each bioreactor, free CALB/GOD/HRP catalyzed cascade reaction was also performed, with dosage of each enzyme was adjusted to the same as that in the corresponding microcapsule bioreactor system. Therefore, the overall efficiency recovery of the three-enzyme reaction will not be affected by the loading amount of enzymes. Table 2 listed relative activities of the six microcapsule bioreactors with CALB/GOD/HRP positional assembled in different strategies.

Obviously, the overall efficiency of the three-enzyme reaction was significantly influenced by the assembly strategies. The lumen(CALB) + shell (GOD)-surface(HRP) (system 1) has the highest activity, while the lumen(HRP) + shell (CALB)-surface(GOD) (system 6) has the lowest value. The difference in catalytic efficiency of microcapsule bioreactors might attribute to differences in the mass transfer of substrates, reaction pathways, and the substrate concentration effect [23,24]. Fig. 4

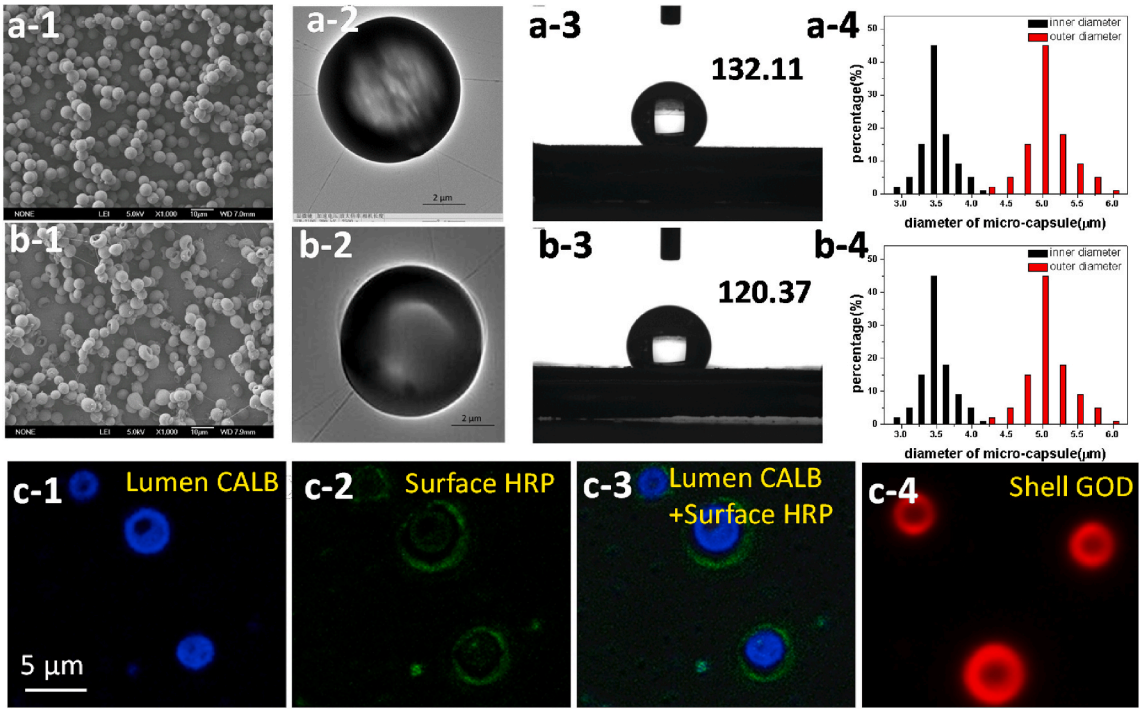

Fig. 3. Characterizations of microcapsules prepared by coaxial electrospray and position assembly of enzymes. (a-1, b-1) SEM images of PU and PAH-doped PU microcapsules; (a-2, b-2). TEM images of PU and PAH-doped PU microcapsules. (a-3, b-3) Images of a water droplet on PU and PAH-doped microcapsules for contact angle measurements. (a-4, b-4) Size distribution of inner and external diameters of PU and PAH-doped microcapsules based on TEM analysis. (c) Confocal laser scanning microscope images of the PAH-doped PU Microcapsule with positionally assembled enzymes. CALB, HRP, and GOD were pre-labeled by Fluorescamine, FITC, and sulforhodamine, respectively, prior to positional assembly. Image in (c-3) is the overlay of (c1) and (c-2).

schematically illustrated the mechanism of the three-enzyme cascade reaction, which involves the generation and subsequent utilization intermediate products, i.e., glucose and H_2O_2, in the multienzyme systems 1 and 6, as examples.

When CALB was encapsulated inside the lumen while HRP assembled on the outer surface of the microcapsules (system 1 shown as Fig. 4a), the primary metabolites product glucose was produced and accumulated inside the aqueous lumen to a high concentration. When glucose diffused out across the shell, it was directly captured and utilized as the substrate of GOD, which was embedded in the shell. Consequently, the secondary metabolites product H_2O_2 was formed and supplied as the substrate of surface-anchored HRP to oxidize the ABTS. Therefore, an ideal cascade reaction route was created and the highest activity was obtained.

When the three enzymes were assembled in the way of lumen (HRP) + shell (CALB)-surface (GOD) (system 6 shown as Fig. 4b), the glucose generated might diffuse in or out across the shell, those diffused out will be captured by surface-attached GOD to generate H_2O_2. Since H_2O_2 was formed on the surface of the microcapsule, most of them will diffuse directly into bulk solution, leaving small amount to diffuse across the shell into the aqueous lumen of the microcapsule, where HRP catalyzed ABTS oxidation takes place. Obviously, diffusional resistance and less efficient capturing/utilization of the primary and secondary metabolites (glucose and H_2O_2) was not conducive to the cascade reaction efficiency; therefore, the system 6 exhibited the lowest overall activity.

The systems 3 and 4 with CALB assembled on the external surface of the microcapsules exhibited activity slightly lower than systems 1 and 2, but much higher than systems 5 and 6. To summarize, we can speculate that the generation of H_2O_2 and its accessibility to HRP was most critical to the overall reaction efficiency. When HRP was assembled on the external surface of the microcapsules (systems 1 and 2), the metabolites H_2O_2 and glucose can be trapped and utilized to the greatest extent.

Table 1
Loading amount and activities of enzyme which was positionally immobilized in PAH-doped PU microcapsule by different strategies.[a].

Enzyme	Position	Enzyme loading(mg/g-microcapsule)	Activity recovery (%)	Specific activity(U/mg-enzyme)	Gross activity(U/g- microcapsule)
CALB	lumen	0.66 ± 0.03	85 ± 1.53	1.82 ± 0.03	1.20 ± 0.05
	shell	0.66 ± 0.04	56 ± 2.53	1.2 ± 0.06	0.79 ± 0.09
	surface	0.68 ± 0.11	76.5 ± 2.53	1.61 ± 0.11	1.09 ± 0.15
GOD	lumen	0.66 ± 0.06	75 ± 0.94	40.5 ± 0.51	26.7 ± 0.27
	shell	0.66 ± 0.08	45 ± 0.94	24.3 ± 0.51	16.1 ± 0.23
	surface	0.12 ± 0.03	71 ± 0.94	38.3 ± 0.06	4.59 ± 0.11
HRP	lumen	0.66 ± 0.05	78 ± 1.04	5.4 ± 0.07	3.56 ± 0.16
	shell	0.66 ± 0.04	48 ± 1.04	3.3 ± 0.07	2.18 ± 0.12
	surface	0.64 ± 0.15	68 ± 1.04	4.67 ± 0.14	2.98 ± 0.14

[a] The immobilization and activity assay of each enzyme was performed separately.

Table 2
Relative activities of microcapsule bioreactors with CALB/GOD/HRP positional assembled in different strategies[a].

No.	Multienzyme system	Loading amount of each enzyme (mg/g-microcapsule)	Schematic diagram	Relative activity for cascade reaction (%)
1	lumen(CALB) + shell (GOD)-surface(HRP)	CALB:0.66; GOD:0.66; HRP:0.64		28.3 ± 0.46
2	lumen(GOD) + shell (CALB)-surface(HRP)	GOD: 0.66; CALB: 0.66; HRP: 0.64		26 ± 0.55
3	lumen(GOD) + shell (HRP)-surface(CALB)	GOD: 0.66; HRP: 0.66; CALB: 0.68		23 ± 2.21
4	lumen(HRP) + shell (GOD)-surface(CALB)	HRP: 0.66; GOD: 0.66; CALB: 0.68		22.5 ± 0.39
5	lumen(CALB) + shell (HRP)-surface(GOD)	CALB: 0.66; HRP 0.66; GOD: 0.12		2.3 ± 0.46
6	lumen(HRP) + shell (CALB)-surface(GOD)	HRP 0.66; CALB: 0.66; GOD: 0.12		1.9 ± 0.46

[a] " , , represent CALB, GOD and HRP, respectively.

3.4. Thermal and operational stabilities of microcapsule bioreactor

The thermal stabilities of microcapsule bioreactor with three-cascade enzymes assembled in the way of lumen (CALB) + shell (GOD)-surface (HRP) (system 1) was determined at 60 °C by detecting changes in the catalytic efficiency of the cascade reaction after storing the microcapsule at this temperature for a different time. It can be seen in Fig. 5a that the free enzyme lost 95% activity within 1 h, whereas the microcapsule bioreactor could maintain more than 50% activity within 5 h under the same conditions, which indicated that immobilized multi-enzyme system is more stable than native enzymes. Operational stability of immobilized biocatalyst is an important feature for its potential applications in industry. Fig. 5 (b) presents the residual activity of the microcapsule bioreactor versus reusing cycles. By defining the initial reaction rate of the first reaction cycle as 100%, it can be seen that the catalytic activity of the microcapsule multi-enzyme bioreactor remained 65% of its original activity during 7 cycles. Considering the enzyme attachment on surface of capsules was mainly driven by weak electrostatic attractions between oppositely charged PAH and the enzyme, the enzymes on the surface of the microcapsule would possibly release slowly during repeated uses, therefore led to decrease in activity. To avoid the release of the enzymes, assembling another negatively charged polyelectrolyte poly(styrene sulfonate) (PSS) would be an effective method [25].

4. Conclusions

A relatively simple method combining the coaxial electrospray, ion pairing of enzyme and layer-by-layer assembly technologies has been developed for the construction of microcapsule-based multi-enzyme cascade reaction system. The PDM prepared by co-axial electrospray has uniform size distribution. The enzyme *in situ* encapsulated inside the aqueous lumen exhibited the highest activity, when compared with that *in situ* embed in the shell or that attached on outer surface of the PDM. By changing the location of each enzyme in the PDM, we were able to investigate the factors influencing the overall efficiency of the cascade reactions. Although the PDM bioreactor presented herein does not provide an inherent catalytic advantage over a mixture of the same enzymes when enzyme cascade was freely dissolved reaction, it clearly provides us a new platform for enzyme precisely assembly and moves the multienzyme assembly in a directed and controlled manner, which enable its potential application in chemical signaling and other related research areas.

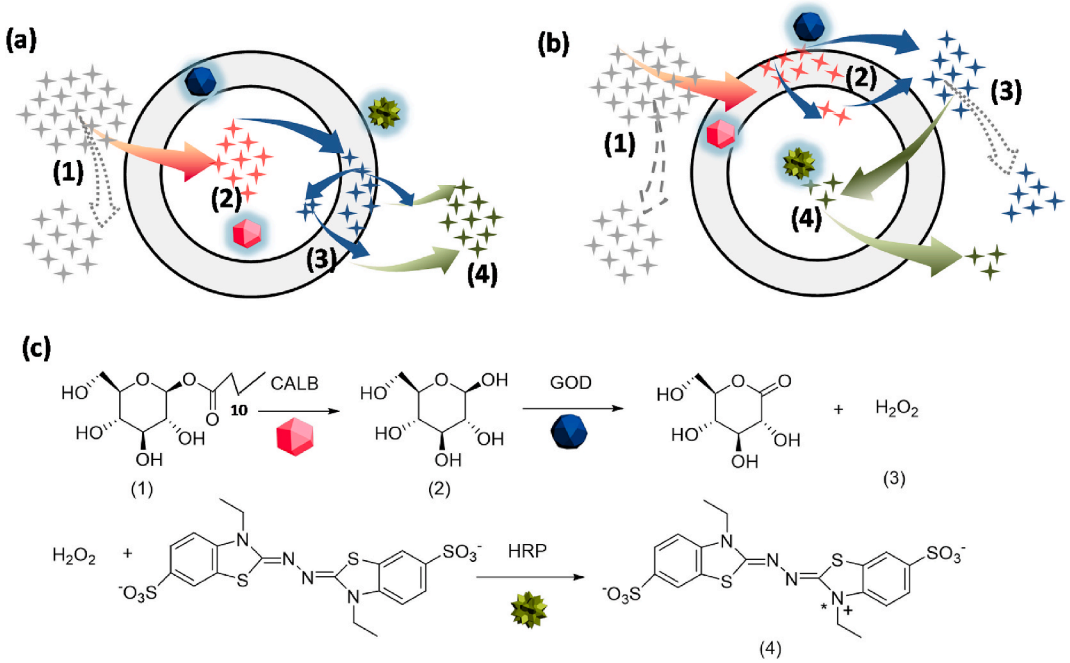

Fig. 4. Schematic illustration of the mechanism of the three-enzyme cascade reaction, which involves the generation and subsequent utilization of intermediate products, i.e., glucose and H_2O_2. (a) Multienzyme systems 1: lumen(CALB) + shell (GOD)-surface(HRP); (b) Multienzyme systems 6: lumen(HRP) + shell (CALB)-surface(GOD); (c) The cascade reaction route, the key substrates and intermediate products shown on (a) and (b) were labeled under the corresponding chemicals.

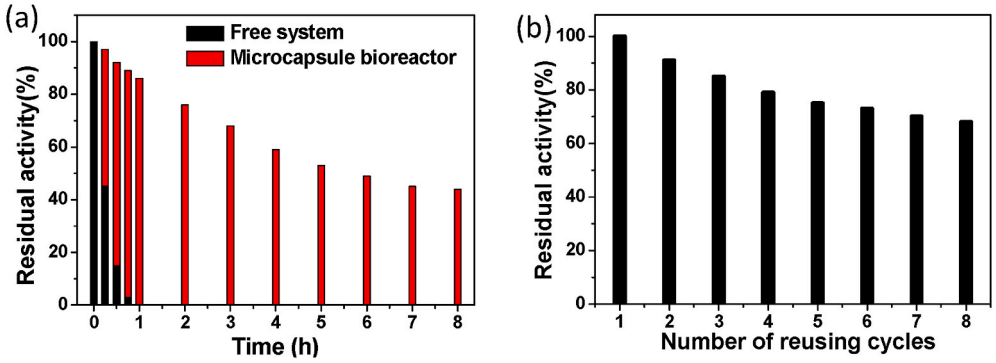

Fig. 5. Performance of microcapsule bioreactor with three-cascade enzymes assembled in the way of lumen (CALB) + shell (GOD)-surface (HRP). a) Thermal stability at 60 °C, and b) reusability of immobilized multi-enzyme systems.

CRediT authorship contribution statement

Shiyi Che: Investigation, Methodology, Writing - original draft, Writing - review & editing. **Jie Wang:** Investigation, Writing - original draft. **Xiaoyuan Ji:** Methodology. **Zhiguo Su:** Supervision. **Shaomin Wang:** Conceptualization, Supervision. **Songping Zhang:** Conceptualization, Supervision, Writing - review & editing.

Declaration of competing interest

The authors declare that they have no known competing financial interests or personal relationships that could have appeared to influence the work reported in this paper.

Acknowledgement

The authors thank the support from the National Natural Science Foundation of China (Grant No. 21676276).

References

[1] Sperl JM, Sieber V. Multienzyme cascade reactions—status and recent advances. ACS Catal 2018;8:2385–96. https://doi.org/10.1021/acscatal.7b03440.
[2] France SP, Hepworth LJ, Turner NJ, Flitsch SL. Constructing biocatalytic cascades: in vitro and in vivo approaches to de Novo multi-enzyme pathways. ACS Catal 2017;7:710–24. https://doi.org/10.1021/acscatal.6b02979.
[3] Schwander T, Schada von Borzyskowski L, Burgener S, Cortina NS, Erb TJ. A synthetic pathway for the fixation of carbon dioxide in vitro. Science 2016;354:900http://science.sciencemag.org/content/354/6314/900.abstract.
[4] Huffman MA, Fryszkowska A, Alvizo O, Borra-Garske M, Campos KR, Canada KA, et al. Design of an in vitro biocatalytic cascade for the manufacture of islatravir. Science 2019;366:1255–9https://www.ncbi.nlm.nih.gov/pubmed/31806816.
[5] Delcea M, Yashchenok A, Videnova K, Kreft O, Möhwald H, Skirtach AG. Multicompartmental micro- and nanocapsules: hierarchy and applications in biosciences. Macromol Biosci 2010;10:465–74. https://doi.org/10.1002/mabi.200900359.
[6] van Dongen SFM, Verdurmen WPR, Peters RJRW, Nolte RJM, Brock R, van Hest JCM. Cellular integration of an enzyme-loaded polymersome nanoreactor. Angew Chem Int Ed 2010;49:7213–6. https://doi.org/10.1002/anie.201002655.
[7] Retterer ST, Simpson ML. Microscale and nanoscale compartments for biotechnology. Curr Opin Biotechnol 2012;23:522–8http://www.sciencedirect.com/science/article/pii/S0958166912000146.
[8] Buddingh BC, van Hest JCM. Artificial cells: synthetic compartments with life-like functionality and adaptivity. Acc Chem Res 2017;50:769–77https://www.ncbi.nlm.nih.gov/pubmed/28094501.
[9] Oberholzer T, Nierhaus KH, Luisi PL. Protein expression in liposomes. Biochem Biophys Res Commun 1999;261:238–41http://www.sciencedirect.com/science/article/pii/S0006291X99904047.
[10] Chang TMS. Semipermeable microcapsules. Science 1964;146:524http://science.sciencemag.org/content/146/3643/524.abstract.
[11] Vriezema DM, Garcia PML, Sancho Oltra N, Hatzakis NS, Kuiper SM, Nolte RJM, et al. Positional assembly of enzymes in polymersome nanoreactors for cascade reactions. Angew Chem Int Ed 2007;46:7378–82. https://doi.org/10.1002/anie.200701125.
[12] Kreft O, Prevot M, Möhwald H, Sukhorukov GB. Shell-in-Shell microcapsules: a novel tool for integrated, spatially confined enzymatic reactions. Angew Chem Int Ed 2007;46:5605–8. https://doi.org/10.1002/anie.200701173.
[13] Shi J, Zhang L, Jiang Z. Facile construction of multicompartment multienzyme system through layer-by-layer self-assembly and biomimetic mineralization. ACS Appl Mater Interfaces 2011;3:881–9. https://doi.org/10.1021/am101241u.
[14] Xue J, Wu T, Dai Y, Xia Y. Electrospinning and electrospun nanofibers: methods, materials, and applications. Chem Rev 2019;119:5298–415https://www.ncbi.nlm.nih.gov/pubmed/30916938.
[15] Lenggoro IW, Xia B, Okuyama K, de la Mora JF. Sizing of colloidal nanoparticles by electrospray and differential mobility analyzer methods. Langmuir 2002;18:4584–91. https://doi.org/10.1021/la015667t.
[16] Ji X, Su Z, Wang P, Ma G, Zhang S. "Ready-to-use" hollow nanofiber membrane-based glucose testing strips. Analyst 2014;139:6467–73https://www.ncbi.nlm.nih.gov/pubmed/25343161.
[17] Ji X, Wang P, Su Z, Ma G, Zhang S. Enabling multi-enzyme biocatalysis using coaxial-electrospun hollow nanofibers: redesign of artificial cells. J Mater Chem B 2014;2:181–90. https://doi.org/10.1039/C3TB21232G.
[18] Ji X, Su Z, Wang P, Ma G, Zhang S. Tethering of nicotinamide adenine dinucleotide inside hollow nanofibers for high-yield synthesis of methanol from carbon dioxide catalyzed by coencapsulated multienzymes. ACS Nano 2015;9:4600–10. https://doi.org/10.1021/acsnano.5b01278.
[19] Ji X, Su Z, Wang P, Ma G, Zhang S. Integration of artificial photosynthesis system for enhanced electronic energy-transfer efficacy: a case study for solar-energy driven bioconversion of carbon dioxide to methanol. Small 2016;12:4753–62. https://doi.org/10.1002/smll.201600707.
[20] Ji X, Su Z, Wang P, Ma G, Zhang S. Polyelectrolyte doped hollow nanofibers for positional assembly of bienzyme system for cascade reaction at O/W interface. ACS Catal 2014;4:4548–59. https://doi.org/10.1021/cs501383j.
[21] Herricks TE, Kim S-H, Kim J, Li D, Kwak JH, Grate JW, et al. Direct fabrication of enzyme-carrying polymer nanofibers by electrospinning. J Mater Chem 2005;15:3241–5. https://doi.org/10.1039/B503660G.
[22] Wang P, Sergeeva MV, Lim L, Dordick JS. Biocatalytic plastics as active and stable materials for biotransformations. Nat Biotechnol 1997;15:789–93. https://doi.org/10.1038/nbt0897-789.
[23] Garcia-Galan C, Berenguer-Murcia A, Fernandez-Lafuente R, Rodrigues RC. ChemInform Abstract: potential of different enzyme immobilization strategies to improve enzyme performance. ChemInform 2012;43. https://doi.org/10.1002/chin.201213261.
[24] Rocha-Martín J, Rivas B, Muñoz R, Guisán JM, López-Gallego F. Rational Co-Immobilization of bi-enzyme cascades on porous supports and their applications in bio-redox reactions with in situ recycling of soluble cofactors. ChemCatChem 2012;4:1279–88. https://doi.org/10.1002/cctc.201200146.
[25] Ji XY, Su ZG, Ma GH, Zhang SP. Sandwiching multiple dehydrogenases and shared cofactor between double polyelectrolytes for enhanced communication of cofactor and enzymes. Biochem Eng J 2018;137:40–9. https://doi.org/10.1016/j.bej.2018.05.017.